Monatsh Chem (2013) 144:1335–1349
DOI 10.1007/s00706-013-1029-0

ORIGINAL PAPER

Edaravone cocrystals: synthesis, screening, and preliminary characterization

Miroslav Veverka · Tibor Dubaj · Ján Gallovič · Emil Švajdlenka · Beáta Meľuchová · Vladimír Jorík · Peter Šimon

Received: 22 October 2012 / Accepted: 31 May 2013 / Published online: 12 July 2013
© Springer-Verlag Wien 2013

Abstract Cocrystals constructed of edaravone (a neuroprotective agent) and phenolic acids (phytochemicals) are investigated. Edaravone and cocrystal formers were coground, slurried, and cocrystallized from solvent at 1:1, 2:1, and 1:2 molar ratios. The physicochemical characteristics of the products were studied using elemental analysis, optical microscopy, Fourier transform infrared spectroscopy, differential scanning calorimetry, and X-ray powder diffraction. Edaravone cocrystals were prepared at various molar ratios. For three cocrystals, i.e., edaravone:gallic acid (2:1), edaravone:protocatechuic acid (1:1), and edaravone:trimesic acid (1:1), two polymorphs have been identified. Representative samples of the cocrystals were exposed to accelerated oxidative and thermal stress to investigate their stability. From the stability screening, protocatechuic acid and gallic acid cocrystals were identified as development candidates because they provide stable cocrystal forms.

M. Veverka · J. Gallovič · E. Švajdlenka · B. Meľuchová
Research and Development Department,
Eurofins Bel/Novamann Ltd.,
820 04 Bratislava, Slovakia

T. Dubaj · P. Šimon (✉)
Faculty of Chemical and Food Technology,
Institute of Physical Chemistry and Chemical Physics,
Slovak University of Technology, Radlinského 9,
812 37 Bratislava, Slovakia
e-mail: peter.simon@stuba.sk

V. Jorík
Faculty of Chemical and Food Technology,
Institute of Inorganic Chemistry, Slovak University
of Technology, Radlinského 9, 812 37 Bratislava, Slovakia

Keywords Nutraceutical · Pharmaceutical cocrystal · Polymorph · Cogrinding · Crystallization · Characterization · Combination drug therapy · Stability

Introduction

Edaravone (ED), 3-methyl-1-phenyl-2-pyrazolin-5-one, a strong free radical scavenger, was developed by Mitsubishi-Tokyo Pharmaceuticals Inc. (Tokyo, Japan). It is used in the treatment of patients with acute brain infarction. ED is an electron donor and when it interacts with free radicals, such as peroxyl radical, the reaction yields corresponding 3-methyl-1-phenylpyrazolin-2,5-dione and 2-oxo-3-phenylhydrazonobutanoic acid. ED blocks both the water-soluble and lipid-soluble peroxyl radical-induced peroxidation systems [1–5]. At present, ED is commercially available as the injection solution in a glass ampoule. From in vitro experiments, Watanabe et al. reported that this formulation is highly reactive toward active oxygen [6–8]. As a consequence of the high affinity for oxygen, an injection formulation of ED in aqueous ethanolic solution should be stabilized with thio-compounds such as pyrosulfate or cysteine [9].

It is more or less accepted that antioxidant substances might be valuable in mitigating neurodegeneration resulting from a transient ischemic event. Oxidative damage is strongly implicated in the pathogenesis of neurodegenerative diseases. Hence, free radical scavengers or chain-terminating antioxidants could prevent the onset or slow down the progression of some, if not most, neurodegenerative conditions. Examples of such antioxidant agents include melatonin, lipoic acid, nonsteroidal anti-inflammatory agents, cysteine, glutathione monoethyl ester, phenolic acids, vitamin E, resveratrol, and flavonoids [10].

Despite the high chance of finding synergy effects, the combination therapy of ED and other drugs has been studied rarely [11–15].

Pharmaceutical cocrystals represent the latest approach to obtain new solid forms of an active pharmaceutical ingredient (API) [16]. Examples of pharmaceutical cocrystals have been demonstrated in the literature to provide improved properties such as physical and chemical stability and thus they can be used as alternative forms of drugs [17, 18]. This paper describes the synthesis and characterization of cocrystals of ED with phenolic acid nutraceuticals as the cocrystal formers (CCFs). Phenolic acids have been reported to possess high antioxidant activity in various systems and some anticarcinogenic activity [19–22]. Pharmaceutical cocrystals of phenolic acids except salicylic acid are relatively marginally explored in terms of solid-state chemistry despite the fact that they contain phenolic groups and the carboxylic acid group serving as a hydrogen bond donor/acceptor [23–28]. The ED:carboxylic acids cocrystals may represent an alternative with the potential for development of combination drug therapy formulations.

The aim of this study was the screening and identification of suitable candidates and assessment of the developability of cocrystal forms of ED in the early development stages. The screening method involved three steps. In the first step, the formation of a cocrystal was verified by applying the simplest and most rapid techniques, i.e., m.p. determination and Fourier transform infrared spectroscopy (FTIR). If the presence of a cocrystal was indicated, the material prepared passed the first step. In the second step, differential scanning calorimetry (DSC) and X-ray powder diffraction (XRPD) measurements were carried out in order to prove the formation of cocrystals. Finally, in the third step, preliminary solid-state stability tests were performed [29–32]. In light of the previously mentioned oxidative instability of the ED injection formulation, oxidative stability of the representative cocrystals against hydrogen peroxide vapor at 30 °C with relative humidity (RH) control was further evaluated [33]. This resulted in a rapid selection of developable cocrystals.

From elemental analysis, FTIR, DSC, and XRPD, novel cocrystals were identified and characterized. Formation of cocrystals with different stoichiometry depends on the experimental procedure [34]; thus, in this study solvent drop grinding (SDG) was compared with solvent cocrystallization (SC) experiments. The systematic study of series of phenolic acids was conducted by the slurring method (SL).

This is a follow-up paper to our previous works [35, 36] dealing with the preparation and characterization of imatinib mesylate cocrystals.

Results and discussion

In order to avoid the solubility limitation and formation of solvates, SDG was the first method of cocrystal preparation. At first, the molar ratio 1:1 was tested, but occasionally the ratios 1:2 or 2:1 were applied for further evaluation and verification of the ratio. Step 1 of screening included simple analytical techniques, i.e., hot-stage microscopy and FTIR, to provide a preliminary indication of potential cocrystal formation. In this way, 14 compounds of three different families, i.e., keto acids, sulfobenzoic acids, and phenolic acids, were screened to cocrystallize with edaravone. The results are shown in Table 1, where positive results (+) from a particular stage of screening indicate the potential interactions. In order to provide a more profound insight into the structural factors that govern cocrystal formation with phenolic acids, systematic slurry preparation of cocrystals has been carried out; the results are summarized in Table 2.

The results of SDG experiments demonstrate the efficiency of the preparation method in 11 out of 14 screening experiments. However, SDG provides the cocrystal with composition corresponding to the stoichiometric ratio of starting materials (1:1) in six out of 11 experiments. This number is difficult to compare with literature data as the number of tested compounds is only occasionally mentioned in the literature. It is noteworthy that in the relatively small number of successful experiments, three new corresponding polymorphs were identified. The solvent crystallization of a 1:1 ingoing ratio of material, sample no. 5, results in the same cocrystallization product with excess unreacted gallic acid (GA); hence, ED:GA (2:1) ratio was expected. The formation of phase-pure ED:GA (2:1) cocrystals was achieved by the SC method in acetonitrile/acetone (1:1) mixture or by SDG when an adequate stoichiometric ratio was applied. In addition, the series of crystallizations from a number of solvents also yielded different polymorphs in the material obtained; FTIR, DSC, and XRPD did not correspond to the aforementioned cocrystal yielded from the SC or SDG method. It was found that the crystallization from ethanol/acetonitrile (1:2) afforded a phase-pure sample with microanalysis data corresponding to the 2:1 cocrystal, but having a different FTIR and DSC records and a new XRPD pattern. Thus, the XRPD pattern corresponds to a new cocrystal ED:GA (2:1) termed here polymorph II. Cocrystal ED:GA (2:1) polymorph II could also be prepared by the slurry crystallization after 1 week of stirring of ingoing components at ambient conditions in cyclohexane or aqueous ethanol. It should be noted that the polymorphism of pharmaceutical cocrystals has been reported relatively rarely [37–44]. Zaworotko investigated the general occurrence of polymorphism in existing cocrystals and found 11 examples [37]. When stoichiometric ratio variations were tested in the SC experiments (samples no. 7, 9) these indeed confirmed the stoichiometric ratios from the SDG results.

Table 1 List of CCFs subjected to screening and m.p., IR, DSC, and XRPD responses after SDG or crystallization with edaravone

No.	Cocrystal former (molar ratio, ED:CCF)	Preparation method	Response				
			m.p.	IR	DSC	XRPD	Stability
1	α-Resorcylic acid (2:1)	SDG, SC, SL	+	+	+	+	nc
2	Citric acid (1:1)	SDG	+	+	am	am	nc
3[a]	Camphanic acid (1:1)	SDG	+	+	+	+	+
4	Ketoglutaric acid (2:1)	SDG, SC	+	+	am	am	nc
5[a]	Gallic acid (2:1) polymorph I	SDG, SC	+	+	+	+	+
6[a]	Gallic acid (2:1) polymorph II	SC, SL	+	+	+	+	+
7	Trimesic acid (1:1) polymorph I	SDG	+	+	+	+	nc
8[a]	Trimesic acid (1:1) polymorph II	SC, SL	+	+	+	+	+
9	Protocatechuic acid (1:1) polymorph I	SDG	+	+	+	+	nc
10[a]	Protocatechuic acid (1:1) polymorph II	SDG, SL	+	+	+	+	+
11	4-Sulfobenzoic acid (1:1)	SDG	+	+	im	+	nc
12[a]	4-Sulfobenzoic acid (2:1)	SDG	+	+	+	+	+
13	4-Sulfobenzoic acid (1:2)	SDG	+	+	im	+	nc
14	Pyrogallol-4-carboxylic acid (1:1)	SL	+	+	+	+	nc

am amorphous phase, *nc* test not conducted, *im* impure sample

[a] Data from these experiments indicate positive responses for all methods and are classified as leads

However, in the course of scale-up studies of the primary SDG method using the SC method from 1:1 ethanol/acetonitrile, the ED:trimesic acid (TMA) (1:1) cocrystal polymorph II was identified.

Generally, SDG experiments were conducted in 5-cm^3 reaction vessels using balls with a diameter of 5 mm. However, in the course of scale-up studies of the SDG method affording the form I of edaravone:protocatechuic acid (PC) (1:1) cocrystal, by applying 20-cm^3 reaction vessels and balls with a diameter of 9 mm another polymorphic form II was prepared. Similar cases are reported, e.g., the effect of the quantity of material on the polymorphic outcome and generation of thermodynamically unstable cocrystals during substantially energetic grinding processes [42, 44].

The identified polymorphs were characterized using FTIR, XRPD, and DSC. Each form exhibits a unique XRPD pattern that differs from the patterns of starting materials (Figs. 1, 2). The melting points of the polymorphs were determined by hot-stage microscopy and verified from the onset temperatures of DSC endothermic peaks (Fig. 3; Table 3). All the polymorphs show unique melting points that differ from those of the starting materials and between them: ED:TMA (1:1) I (200.1 °C), ED:TMA (1:1) II (208.4 °C), ED:PC (1:1) I (116.4 °C), ED:PC (1:1) II (114.4 °C), ED:GA (2:1) I (154.4 °C), ED:GA (2:1) II (146.4 °C). The fact that a higher number of polymorphs were prepared in small series of cocrystals suggests the importance of polymorph screening of cocrystals and raw materials and their thorough characterization. Polymorphs can usually be discriminated using DSC data from the onset of melting and heats of fusion or by the infrared rule [45]. As stated by the heat of fusion rule, a higher melting form has a higher heat of fusion in a monotropic system and a lower heat of fusion in an enantiotropic system. In the case of ED:PC cocrystal, the polymorph I with higher melting temperature has a higher heat of fusion; it can be concluded that the polymorph I is a monotrope. Likewise, in the case of ED:TMA form II, higher melting forms have higher heats of fusion. The relative stability of the two polymorphs of the ED:PC (1:1) cocrystal was studied by placing a mixture of crystals of form I and form II in open glass vials at 40 °C with 75 % RH; no transformation was observed after 2 months by DSC and the 1:1 cocrystal mixture showed two unchanged endothermic events at onset temperatures of 116.4 °C (128 J/g) and 114.4 °C (124 J/g) for the polymorphs I and II, respectively. This result gives evidence that in this range of temperature and RH both polymorphs I and II are stable.

The thermodynamic relationships between polymorphs I and II of ED:GA (2:1) respectively could be enantiotropically related. Relative polymorph stabilities for ED:GA cocrystals were deduced from SL cocrystallization in two solvents; where after 1 week form II was confirmed as remaining solid, meanwhile the themodynamically unstable form I was obtained by energetic grinding [42]. The FTIR spectra of forms I and II of ED:GA (2:1) cocrystals are presented in Fig. 4. Absorption peaks in the $\approx$1,670 cm^{-1} region correspond to carbonyl group vibrations of gallic acid. Other differences between the IR spectra of the polymorphs are present in the regions 740–760, 1,150–1,180, 1,400–1,420, 1,550–1,560, and

Table 2 Overview of SDG, SC, and SL cocrystal formation experiments of edaravone with phenolic acids

CCF	Method		
	SDG (molar ratio)	SC (molar ratio)	SL (molar ratio)
2-Hydroxybenzoic acid	− (1:1, 2:1, 1:2) DMF	− (1:1, 2:1, 1:2) ET	− (1:1) AN, AE, W
	− (1:1, 2:1, 1:2) W	− (1:1, 2:1, 1:2) AN	− (1:2) AN, W, AE
	− (1:1, 2:1, 1:2) AN	− (1:1, 2:1, 1:2) BU	− (2:1) AN, W, AE
3-Hydroxybenzoic acid (3HB)	− (1:1, 2:1, 1:2) DMF	− (1:1, 2:1, 1:2) AN	− (1:2) CH, W, AE
	− (1:1, 2:1, 1:2) W	− (1:1, 2:1) ET, AN	− (2:1) W, AE
	− (1:1, 2:1, 1:2) AN		− (1:1) AE, W, CH
4-Hydroxybenzoic acid (4HB)	− (1:1, 2:1, 1:2) DMF	− (1:1, 2:1, 1:2) AN	− (2:1) W, AE
	+ **(2:1)** W	− (1:1, 2:1, 1:2) ET	− (1:1) AE, W, CH
	− (1:1, 2:1, 1:2) AN		
2,3-Dihydroxybenzoic acid	− (1:1, 2:1, 1:2) DMF		− (2:1) W, AE
	− (1:1, 2:1, 1:2) W		− (1:1) AE, W, CH
	− (1:1, 2:1, 1:2) AN		
2,5-Dihydroxybenzoic acid	− (1:1, 2:1, 1:2) DMF	− (1:1, 2:1, 1:2) ET	− (2:1) CH
	− (1:1, 2:1, 1:2) W	− (1:1, 2:1, 1:2) AN	+ **(1:1)** AE
	− (1:1, 2:1, 1:2) AN		
3,4-Dihydroxybenzoic acid (PC)	+ **(1:1)**, − (2:1, 1:2) DMF	+ **(1:1)** AC-AN	+ **(1:1)** AE
	+ **(1:1)**, − (2:1, 1:2) W	+ **(1:1)** ET-AN	− (1:1) CH
	+ **(1:1)**, − (2:1, 1:2) AN		
3,5-Dihydroxybenzoic acid (RA)	+ **(2:1)**, − (1:1, 1:2) DMF		− (1:1) CH
	+ **(2:1)**, − (1:1, 1:2) W		+ **(2:1)** W
	+ **(2:1)**, − (1:1, 1:2) AN		+ **(2:1)** AE
2,4,6-Trihydroxybenzoic acid	− (1:1, 2:1, 1:2) DMF	− (1:1, 2:1, 1:2) AN	− (1:1, 1:2) AN,
	− (1:1, 2:1, 1:2) W		− (2:1) AN
	− (1:1, 2:1, 1:2) AN		
2,3,4-Trihydroxybenzoic acid (PG)	− (1:1, 2:1, 1:2) DMF		+ **(1:1)** AE
	− (1:1, 2:1, 1:2) W		− (1:1) W
	− (1:1, 2:1, 1:2) AN		− (2:1) CH, W, AE
3,4,5-Trihydroxybenzoic acid (GA)	+ **(2:1)**, − (1:1, 1:2) DMF	+ **(2:1)** AC-AN	+ **(2:1)** CH
	+ **(2:1)**, − (1:1, 1:2) W	+ **(2:1)** ET-AN	+ **(2:1)** AE
	+ **(2:1)**, − (1:1, 1:2) AN		
m-Coumaric acid	− (2:1, 1:1) W		− (1:1) W, AE
	− (2:1, 1:1) AN		
	− (1:1, 2:1, 1:2) DMF		
Caffeic acid	− (2:1, 1:1, 1:2) AN		− (1:1) W, AE
	− (2:1, 1:1) W		− (2:1) W, AE
	− (1:1, 2:1, 1:2) DMF		

+ sign denotes the cocrystal formation (stoichiometry highlighted in bold); − sign denotes a mixture of the starting materials without a cocrystal formation

AC acetone, *AE* (1:1, v/v) aqueous ethanol solution, *AN* acetonitrile, *BA* butyl acetate, *BU* butanol, *CH* cyclohexane, *Cl* chloroform, *DMF* dimethylformamide, *ET* ethanol, *W* water

3,200–3,360 cm^{-1}. The absorption peak relation between the two polymorphs located in the $\approx$1,670 cm^{-1} region appears to be in accordance with Burger and Ramberger's infrared rule, which states that the phase I that absorbs at higher frequencies is less stable at 0 K [45].

We further investigated cocrystal formation of edaravone with SBA and TMA. From a crystal engineering view, SBA and TMA are CCFs with higher molecular complexity, TMA with its threefold symmetrically disposed carboxyl groups and SBA with two nonequivalent acidic groups. This stimulated us to construct supramolecular architectures of ED and SBA, which would be expected to exhibit diversified hydrogen-bonding modes and interesting architectures [46]. Only the SDG method afforded a phase-pure cocrystal ED:SBA in the stoichiometric ratio 2:1. DSC records also indicated the presence

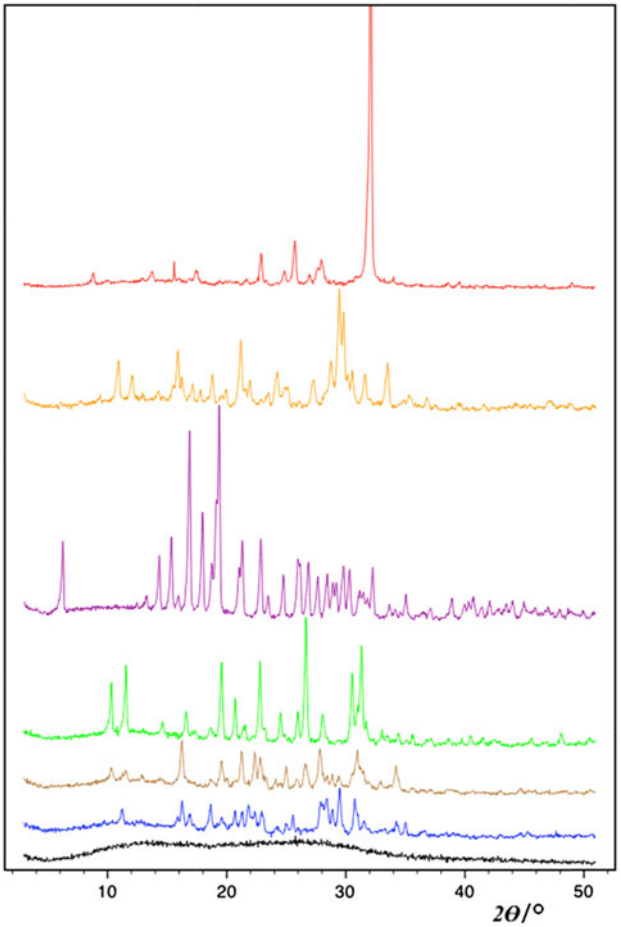

Fig. 1 XRPD patterns for (from *top* to *bottom*) ED:TMA (1:1) polymorph II, ED:TMA (1:1) polymorph I, ED:CA (1:1), ED:4-sulfobenzoic acid (SBA) (2:1), ED:SBA (1:1), ED:SBA (1:2), ED:KG (2:1) cocrystals

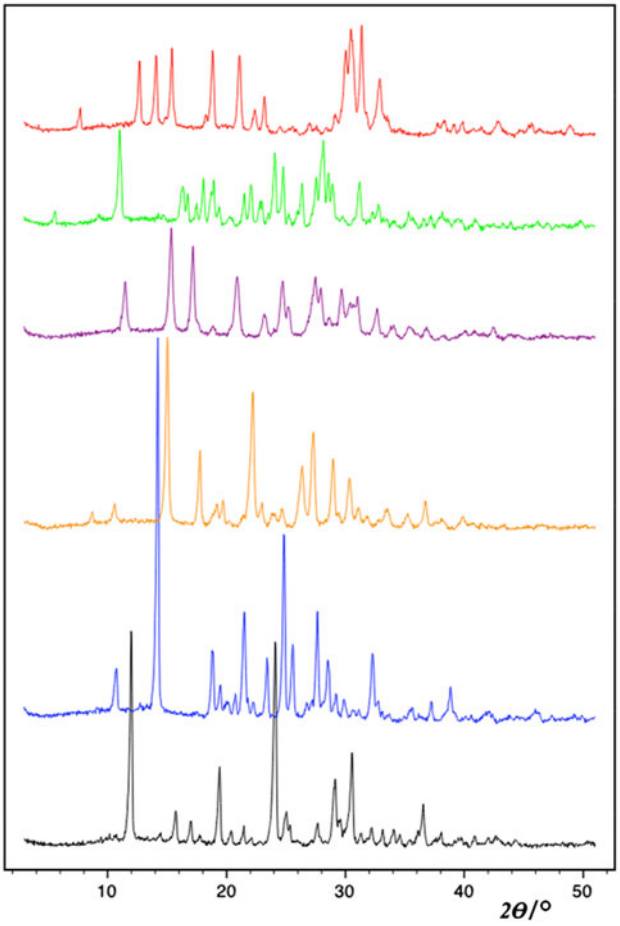

Fig. 2 XRPD patterns for (from *top* to *bottom*) ED:PC (1:1) polymorph I, ED:PC (1:1) polymorph II, ED:RA (2:1), ED:GA (2:1) polymorph I, ED:GA (2:1) polymorph II, ED:PG (1:1) cocrystals

of new phase via the SDG method for 1:1 and 1:2 stoichiometry; ED and SBA were consumed and a smaller amount of impurity was detected alongside with traces of solvent (Fig. 3). But, the different XRPD patterns of three resulting structures (Table 1, samples no. 8, 9, 10) were observed as presented in Fig. 1. However, these samples were excluded from the next screening. The variations of stoichiometry were unexpected and we hypothesized that the sulfonic group can be complexed, too. Cocrystal sulfonates and their single-crystal structure determinations have been reported rarely and mimicking of a carboxylic group was confirmed [47–50]. Unfortunately, in our case a single crystal of this structure for the single-crystal XRD measurement was not obtained. As stated above the cocrystal of ED:TMA 1:1 using SDG afforded polymorph I and the SC method afforded polymorph II. These examples illustrate another case in which the different methods produce different cocrystal polymorphs.

The first stage of screening identified two materials by melting point and FTIR that were then identified as amorphous by DSC and XRPD methods. This is observed during grinding [51, 52] as is true for ED:citric acid (1:1) cocrystal. Pure citric acid monohydrate (CIT) has bands at 1,721 and 1,685 cm^{-1} corresponding to the ν(COOH) and (C=O) stretch. During the formation of ED:CIT (1:1) cocrystal these bands were shifted to 1,698 and 1,678 cm^{-1} as weak broad bands, which indicated the formation of hydrogen bonding. However, the XRPD pattern revealed that the material was obtained as an amorphous solid. On the other hand, ED:ketoglutaric acid (2:1) cocrystals precipitated as a glassy (softening around 130 °C) material from an ethanol/acetonitrile (9:1, v/v) system. To examine the effect of solvents on the solid state of the aforementioned materials, we took the same measurements on the samples from SC using various solvents including acetonitrile, acetone, 2-methyl-2-butanol, methyl ethyl ketone, dipropyl ether, butyl acetate, and chloroform [53]. In solvent treatments mentioned above, if a solid material precipitated, we found that we got the identical amorphous material using different solvents. No peaks were observed

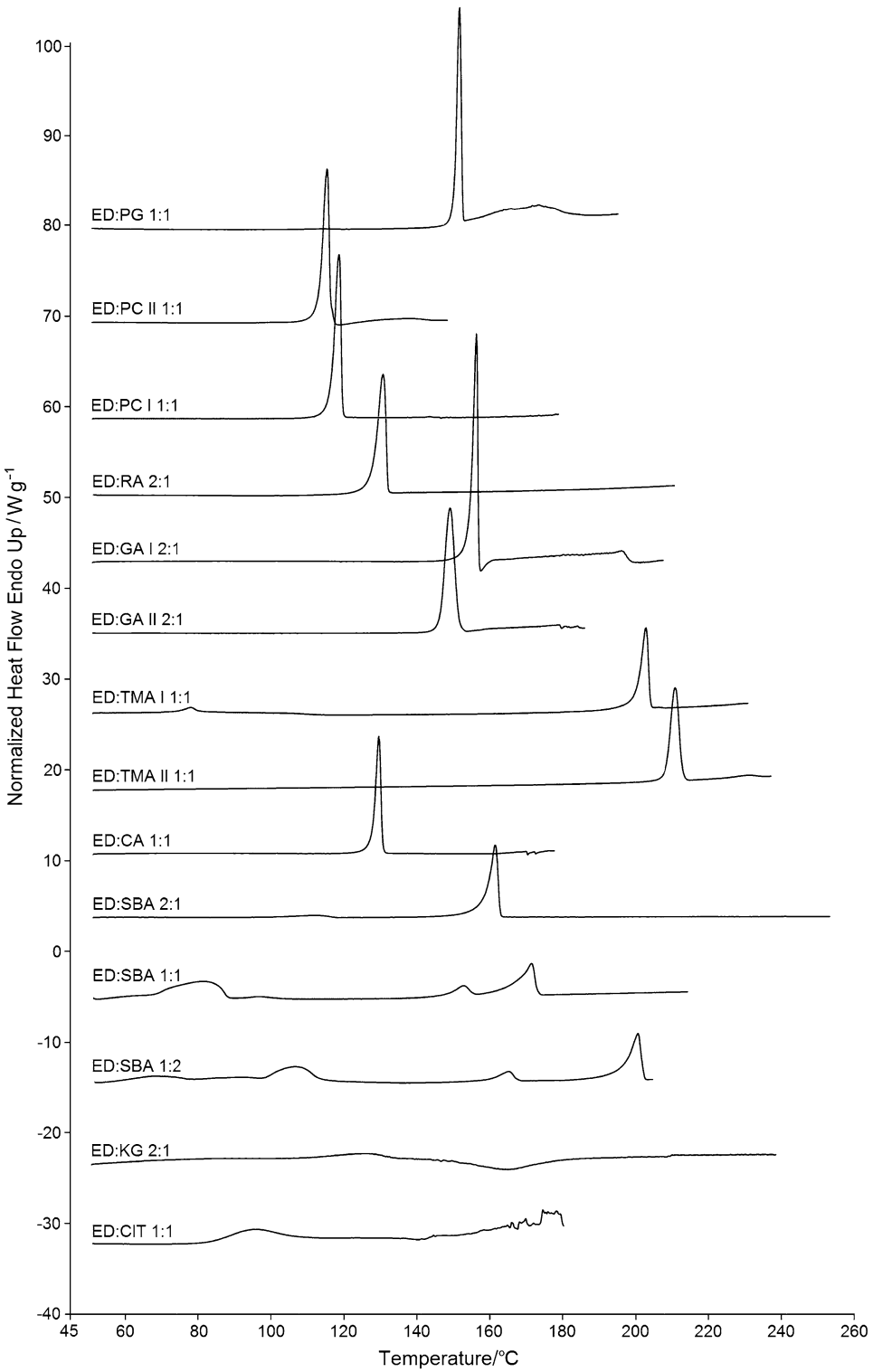

Fig. 3 DSC curves of (from *top* to *bottom*) ED:PG (1:1), ED:PC (1:1) polymorph II, ED:PC (1:1) polymorph I, ED:RA (2:1), ED:GA (2:1) polymorph I, ED:GA (2:1) polymorph II, ED:TMA (1:1) polymorph I, ED:TMA (1:1) polymorph II, ED:CA (1:1), ED:SBA (2:1), ED:SBA (1:1), ED:SBA (1:2), ED:KG (2:1), ED:CIT (1:1) cocrystals

in XRPD patterns except for a halo-like pattern at 2θ between 10° and 25° confirming its amorphous state (Fig. 1). As we are not interested in amorphous forms, ED:CIT (1:1) and ED:KG (2:1) materials were rejected as development candidates and excluded from the next stage of screening.

Unexpectedly, in the case of salicylic acid as CCF the FTIR and DSC clearly show that no cocrystal is formed. Following from these negative observations, the synthesis of cocrystals was attempted by SDG, SC, or the SL method from other structurally related phenolic acids. As non-bonding interactions in cocrystals take place, a steric

Table 3 Melting points and DSC data of the edaravone cocrystals

Cocrystal former (molar ratio, ED:CCF)	m.p./°C	T_{onset}/°C	$\Delta_{fus}H$/J g^{-1}	CCF, T_{onset}/°C
Edaravone	127–129	128.0	151.6	–
α-Resorcylic acid (2:1)	126–127	127.8	126.5	235.1
Citric acid (1:1)	~103	am	–	151.6
Camphanic acid (1:1)	123–124	127.9	129.4	204.7
Ketoglutaric acid (2:1)	≈130	am	–	114.2
Gallic acid (2:1) I	154–155	154.4	124.8	259.1
Gallic acid (2:1) II	144–146	146.4	135.1	259.1
Trimesic acid (1:1) I	>235^{dec}	200.1^{dec}	78.0^{dec}	361.5^{dec}
Trimesic acid (1:1) II	>215^{dec}	208.4^{dec}	93.3^{dec}	361.5^{dec}
Protocatechuic acid (1:1) I	114–115	116.4	128.3	202.2
Protocatechuic acid (1:1) II	111–113	114.4	123.7	202.2
4-Sulfobenzoic acid (1:1)	163–170	im	–	≈99
4-Sulfobenzoic acid (2:1)	155–158	158.7	86.2	≈99
4-Sulfobenzoic acid (1:2)	200–202	im	–	≈99
Pyrogallol-4-carboxylic acid (1:1)	158	151.9	112.2	214.1

dec decomposition, *im* impure sample, *am* amorphous phase

arrangement of hydroxyl moieties seems to be important. From the results mentioned above we deduced that the presence of the 3-hydroxyl moiety in benzoic acids leads to interaction with ED; therefore 3-hydroxybenzoic acid (3HB), 3,5-dihydroxybenzoic acid (α-resorcylic acid, RA), and 2,3,4-trihydroxybenzoic acid (pyrogallol-4-carboxylic acid, PG) were tested as CCFs. Indeed, the corresponding cocrystal (sample 1, Table 1) was prepared by SDG, SL, or the SC method at the stoichiometry 2:1 ED:RA. All the cocrystals obtained by SDG are reproduced by SL; however, ED:PG (1:1) cocrystals were obtained solely by SL, and thus slurry cocrystallization seems more effective. For 3-hydroxybenzoic acid the FTIR method indicated a new phase and DSC showed a clear single melting peak (92 °C). Additional mixtures were prepared to verify the formation of the eutectic mixture. However, all of the materials with the 2:1, 1:2, or 1:1 ratio show the same eutectic point thereby indicating the absence of cocrystal formation (Fig. 5). Also, the XRPD patterns of these materials showed negligible differences against the patterns of starting compounds; so the formation of cocrystal did not take place.

Phenolic acids occasionally showed surprising results, as two stoichiometrically different cocrystals were isolated [18, 53, 54]. The cocrystals obtained from a pair of isomeric dihydroxybenzoic acids (3,5- vs. 3,4-dihydroxy) and trihydroxybenzoic acids (3,4,5- vs. 2,3,4-trihydroxy) exhibit different stoichiometric ratios of 2:1 vs. 1:1. It was found that the SL method afforded a cocrystal with appropriate stoichiometry (Table 2) regardless of the used ongoing ratio (1:1, 1:2, 2:1) of starting materials. According to the aforementioned idea we tested caffeic acid and 3-hydroxycinnamic acids using the slurry cocrystallization; no cocrystal formed. Table 2 summarizes the cocrystals prepared from hydroxybenzoic acids by the slurry method. This behavior of hydroxyl benzoic acids has already been reported. Broad screening of acetazolamide with many structural isomers of hydroxybenzoic acids yielded a cocrystal only for 4-hydroxy- and 2,3-dihydroxybenzoic acid [28].

The melting points were compared with those of the ED and CCFs. The melting points of obtained samples are diffused; however, they fell mostly between the values of edaravone (127–129 °C) and the corresponding CCF. The distinct melting points of cocrystals clearly indicate the formation of a new crystalline phase. These cocrystals were shown to alter the melting point of edaravone, suggesting that physical properties of great pharmaceutical relevance, e.g., solubility and thermal stability, have been altered. In this series, however, no direct correlation between melting points of either individual component and that of the cocrystal could be found. The FTIR spectra of representative cocrystals are depicted in Figs. 6 and 7. Use of FTIR was possible through the inclusion of a set of physical mixtures of edaravone and CCFs representing possible solid-state outcomes from the cocrystal screening. The tendency of CCFs to interact with edaravone is demonstrated in Table 1. FTIR spectra of cocrystals compared with those of the pure compounds or their physical mixture showed numerous changes. It can be seen that for cocrystals, the characteristic peaks either reduced their intensity, disappeared, shifted, or new peaks appeared (Fig. 4). Indeed, most of the peaks of CCFs shifted in this way, e.g., the C=O stretching vibration of the carboxylic group at 1,728 cm^{-1} for camphanic acid occurred at 1,674 cm^{-1} in ED:CA (1:1) cocrystal. An increase in the frequency of the keto group of camphanic acid was observed from 1,745 to 1,782 cm^{-1} in ED:CA (1:1) cocrystal (Table 4). An

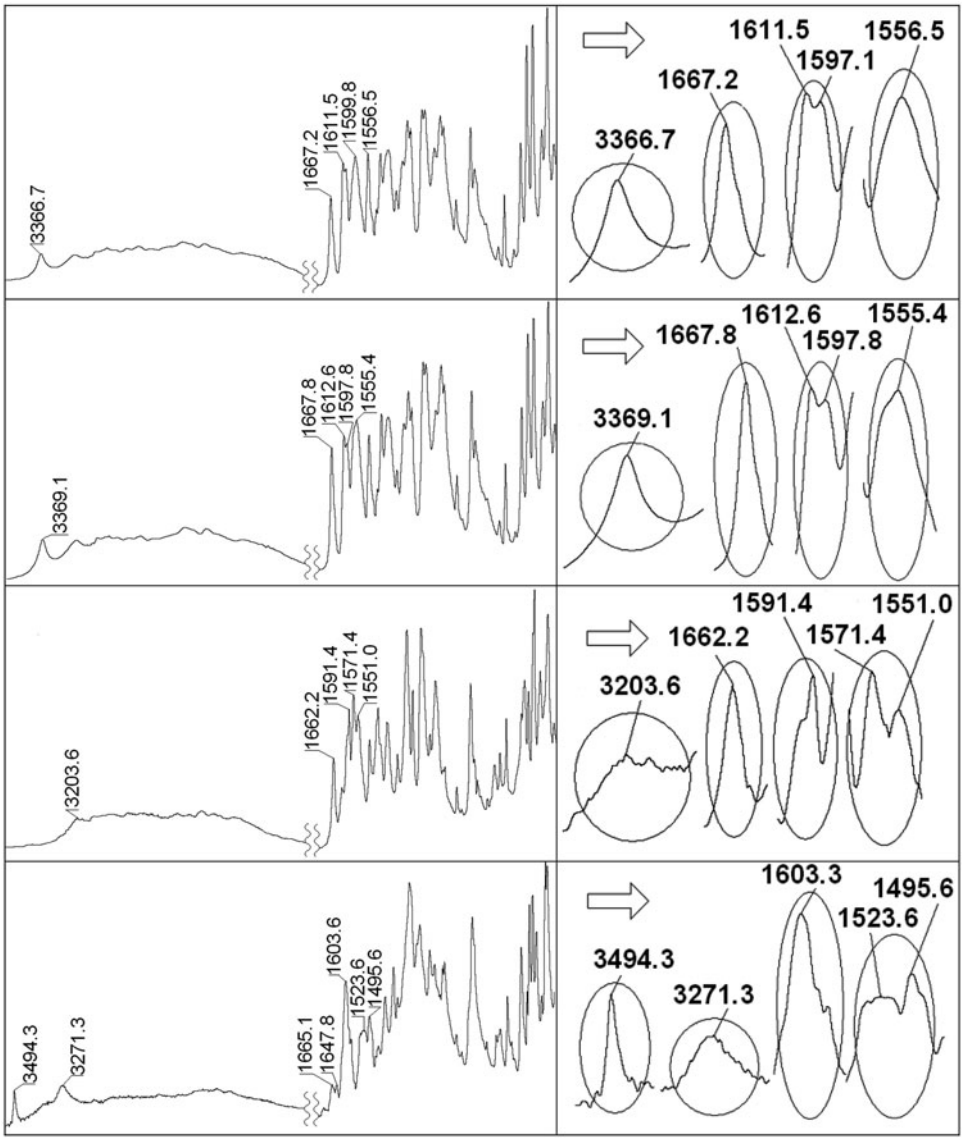

Fig. 4 Example of FTIR spectra used to identify potential cocrystals (from *top* to *bottom*): ED:GA (2:1) polymorph I, prepared by SC; ED:GA (2:1) polymorph I, prepared by SDG; ED:GA 2:1 polymorph II, prepared by SC; GA and ED physical mixture

increase in the frequency of the keto group of camphanic acid was observed from 1,745 to 1,782 cm^{-1}. The IR spectrum of pure ketoglutaric acid (KG) and CIT starting material shows characteristic peaks attributed to the *v*(COOH) and (C=O) stretch, respectively. During cocrystallization these bands were shifted which indicates that the carboxyl group is participating in hydrogen bonding. However, the situation for these ED:polycarboxylic acids (1:1) systems was somewhat unclear. The IR spectrum shows an indistinguishable broad multiplet at $\approx$1,705 cm^{-1}, and the new absorption bands attributable to *v*(COOH) group were strongly overlapped with the mostly unperturbed COOH absorption bands. For all other tested acids, however, the carbonyl peak occurred at 1,715–1,682 cm^{-1} clearly in agreement with the structural evidence for the cocrystal formation. Also, a new band at 1,596 cm^{-1} attributed to the C=N of the edaravone skeleton appeared. This band appeared only in those cases where edaravone was found to form the cocrystal.

Crystal morphology and particle size are important for handling the drug substance and for reliable manufacture of dosage forms with uniform drug content. The optical micrographs of representative cocrystals are shown in Fig. 8. The morphology of the cocrystals ranges from a rhombic habit for **8a** (mean value 450 μm, ED:GA (2:1), polymorph II), to a hexagonal morphology with irregular surface for **8b**, **8d** and tetragonal prism for **8c** [mean value 270 μm, ED:TMA (1:1)]. Form ED:GA (2:1), polymorph II is particularly easy to filter and dry to a free-flowing powder.

DSC experiments were carried out to study the thermal behavior of ED cocrystals in relation to the individual components. The DSC records and m.p. for ED, individual native CCFs, and cocrystals were compared. The DSC

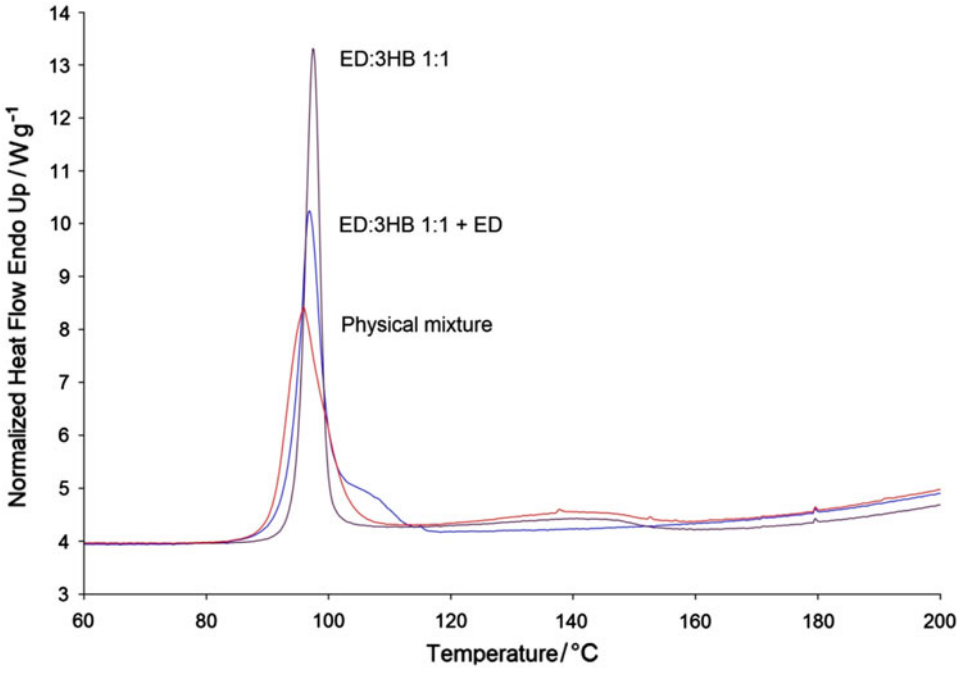

Fig. 5 DSC records of (from *top* to *bottom*) potential cocrystal ED:3HB (1:1) by the SL method, potential cocrystal ED:3HB (1:1) by the SL method doped with ED, and the physical mixture ED:3HB (1:1)

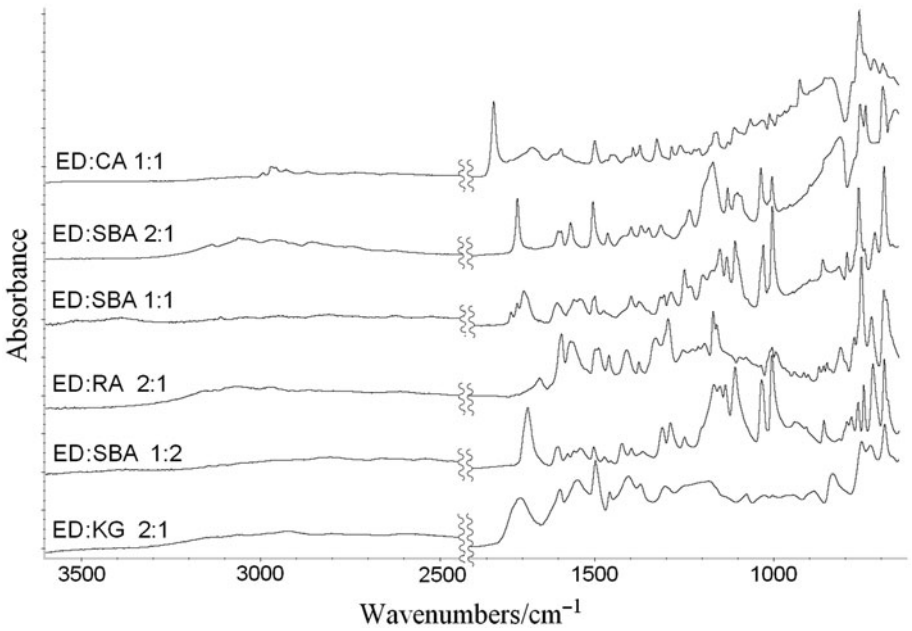

Fig. 6 FTIR spectrum of (from *top* to *bottom*) ED:CA (1:1), ED:SBA (2:1), ED:SBA (1:1), ED:RA (1:1), ED:SBA (1:2), ED:KG (2:1) cocrystals

records are shown in Fig. 3; the melt endotherms obtained from the DSC data are shown in Table 3, with the melting points for the corresponding cocrystal components. The DSC results revealed significant differences between the values of the melting point onsets of pure ED and ED cocrystals. This melting point mostly occurs between the melting points of the starting materials (ED at 127–129 °C and CCFs). Formation of the cocrystal then results in increased thermal stability of ED, but a lower stability for the CCFs molecules. A single endothermic peak for co-crystals indicates the absence of any unbound or absorbed solvent and demonstrates the stability of phase until the

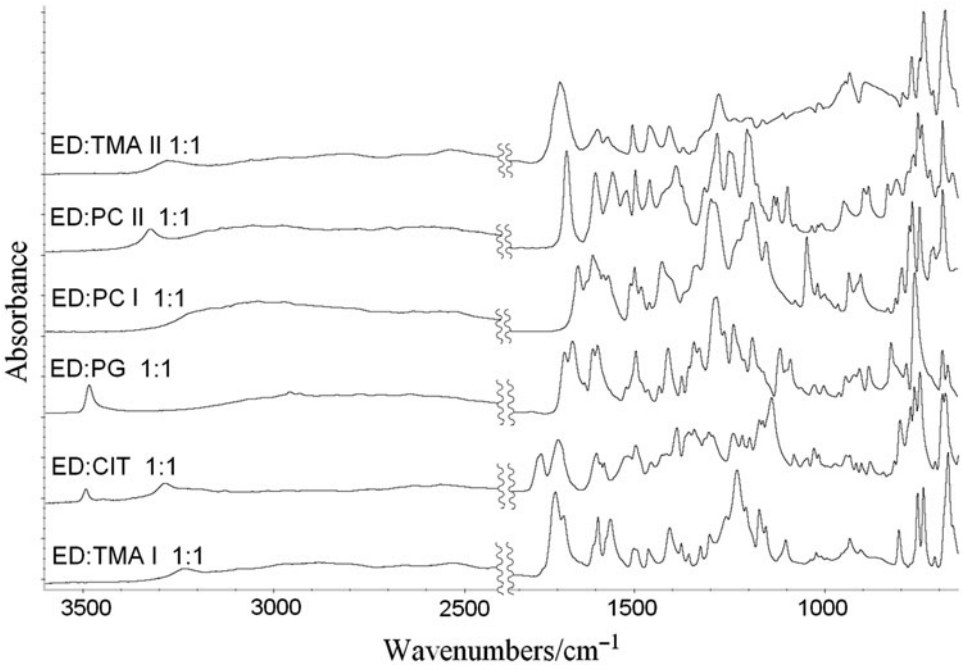

Fig. 7 FTIR spectrum of (from *top* to *bottom*) ED:TMA (1:1) polymorph II, ED:PC (1:1) polymorph II, ED:PC (1:1) polymorph I, ED:PG (1:1), ED:CIT (1:1), ED:TMA (1:1) polymorph I cocrystals

Table 4 Assignment of the major bands of the infrared spectra of cocrystals

No.	Cocrystal former (molar ratio, ED:CCF)	ν(COOH)/cm^{-1}	ν(C=N$_{het}$)/cm^{-1}	ν(OH) of COOH/cm^{-1}
1	α-Resorcylic acid (2:1)	1,653	1,592	1,409
2	Citric acid (1:1)	1,698	1,598	1,420
3	Camphanic acid (1:1)	1,674	1,594	1,391
4	Ketoglutaric acid (2:1)	1,705	1,596	1,403
5	Gallic acid (2:1) polymorph I	1,668	1,597	1,411
6	Gallic acid (2:1) polymorph II	1,662	1,591	1,419
7	Trimesic acid (1:1) polymorph I	1,686	1,594	1,406
8	Trimesic acid (1:1) polymorph II	1,691	1,596	1,407
9	Protocatechuic acid polymorph I (1:1)	1,682	1,595	1,411
10	Protocatechuic acid polymorph II (1:1)	1,677	1,601	1,389
11	4-Sulfobenzoic acid (1:1)	1,697	1,603	1,397
12	4-Sulfobenzoic acid (2:1)	1,715	1,600	1,397
13	4-Sulfobenzoic acid (1:2)	1,686	1,601	1,397
14	Pyrogallol-4-carboxylic acid (1:1)	1,646	1,607	1,407

melting point. For ED:SBA (1:1, 1:2) cocrystals, however, the DSC of the cocrystal indicated traces of CCF. When CIT or KG was applied, the DSC traces clearly indicate an amorphous phase. There are several suggestions found in the literature that cogrinding induces an amorphization [51, 52]. The amorphous samples of ED:CIT and ED:KG cocrystals were aged at 25 °C with 35 % RH, for 2 months, to assess the effect of storage on their crystallizability. Cocrystals ED:CIT and ED:KG solidified but the repeated DSC measurements did not detect any crystalline phase.

A different XRPD pattern for each ED cocrystal confirms the formation of a new cocrystal phase; a unique XRPD pattern enables unambiguous distinction between the cocrystals from ED and CCFs. As stated above, only the samples with indubitable XRPD patterns from the screening experiments were classified as positive. The XRPD patterns of cocrystals are shown in Figs. 1 and 2. The low-angle region at $2\theta = 5°–30°$ was used to reliably distinguish between various crystal forms of new cocrystals. The XRPD patterns revealed that the formation of cocrystals via SDG occurred with stoichiometric ratios corresponding to the starting materials; no starting material was detected except SBA. Total consumption of starting ED and unused CCFs was revealed by XRPD in some cases. Finally, using appropriate stoichiometric variation (e.g., ED:GA 2:1), the desired cocrystals were obtained and

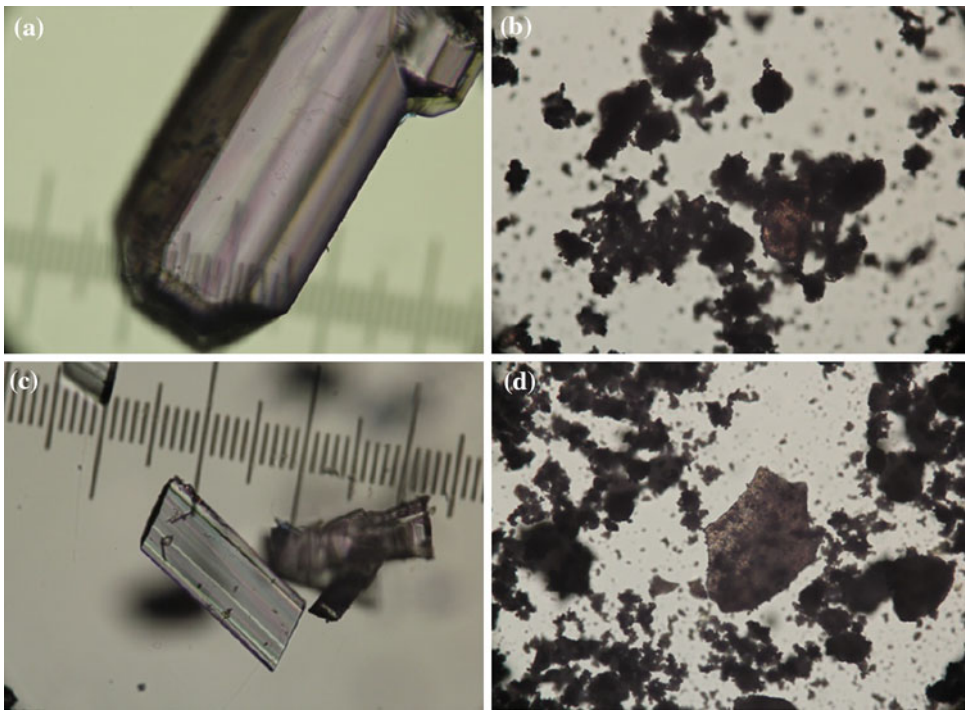

Fig. 8 Optical micrographs of **a** ED:GA (2:1) polymorph II, **b** ED:GA (2:1) polymorph I, **c** ED:TMA (1:1) polymorph II, **d** ED:TMA (1:1) polymorph I prepared by SC (*left*) or SDG (*right*)

confirmed by XRPD. The new XRPD patterns were found to correspond to polymorphs of cocrystals ED:GA, ED:TMA, and ED:PC.

Stability tests as a function of time versus humidity and temperature are useful in assessing the shelf life of cocrystals. Thus, cocrystals were subjected to temperature 40 °C and 75 % RH for 2 months. The solids were analyzed by m.p., FTIR, DSC, and XRPD and compared with unstressed samples to confirm a physical stability. Cocrystals displayed physical stability; no recognizable differences in m.p. and the FTIR, DSC, and XRPD patterns were found. The type of polymorphic form does not have a significant influence on the stability under the testing conditions. As an example, the XRPD patterns for ED:PC (1:1) cocrystals before and after exposure are shown in Fig. 9. It can be seen that any significant change indicating decomposition in the patterns did not occur. The intensity of diffraction peaks in the stressed samples was somewhat different compared with the starting material owing to a diverse measurement condition (sample volume). Thermal stability/relative humidity results (TS) are summarized in Table 5.

The next stage, i.e., the oxidative-stability screening, also provides additional information regarding the stability. Edaravone is thermally stable; however, peroxide vapor-mediated oxidation was confirmed under the test conditions with unidentified degradants as monitored by HPLC. Edaravone, as a blank, showed significant decrease of the content to 89.8 % during exposure to hydrogen peroxide vapor. Thus, the cocrystal solid samples were exposed in

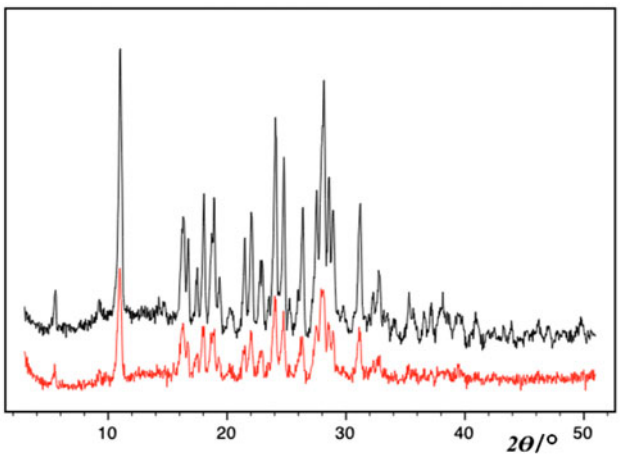

Fig. 9 XRPD patterns for (from *top* to *bottom*) cocrystal ED:PC (1:1) polymorph II and cocrystal ED:PC (1:1) polymorph II after exposure

parallel using the condition 25 °C/65 % RH for 3 days. Generally, the tested cocrystals maintain a practically unchanged content of ED. This preliminary study indicates that stabilization is probably a result of the beneficial effect of CCF. These experimental results demonstrated that the proposed antioxidant protection can be used to generate stable products and is useful for the development of drug products; the results are summarized in Table 5.

In the final stage of stability screening, sorption of water was conducted to identify "developable" cocrystal candidates. Water sorption for selected cocrystals was determined at 25 °C and 55, 80, and 90 % RH. The

Table 5 HPLC data and stability results for ED and representative cocrystals

Sample	OS	WS	TS
ED	89.8 (area %)	+	nc
ED:CA (1:1)	+	+	+
ED:PC (1:1) polymorph II	+	+	+
ED:SBA (2:1)	+	+	+
ED:TMA (1:1) polymorph II	+	+	+
ED:GA (2:1) polymorph I	+	+	+

OS oxidation stability, + no decrease in content with respect to ED, *WS* water sorption, + change in mass <0.1 %, *TS* solid-state stability with respect to temperature and relative humidity, + test passed, *nc* test not conducted

cocrystal was regarded as non-hygroscopic if it sorbed less than 0.1 % water even at high humidity; the results for 90 % RH are summarized in Table 5. It was evident that ED cocrystals sorbed a negligible amount of water (≪0.1 %), practically the same as a ground sample of ED. These preliminary results indicate that the ED cocrystals are non-hygroscopic. Generally, all tested materials had satisfactory thermal and oxidation stability and did not undergo hydration under increased humidity.

The dissolution curves almost perfectly obeyed first-order kinetics (Fig. 10). Purely formally (without considering mechanistic details such as the solution-mediated transformation and solute–solute interaction), the dissolved concentration c can be expressed as

$$c = c_{\infty}[1 - \exp(-kt)] \quad (1)$$

where c_{∞} is the final concentration, k is the dissolution rate constant, and t stands for time.

Since the final concentration is unknown, for the treatment of dissolution data non-linear regression was employed; the results are presented in Table 6.

The dissolution tests were conducted to compare the dissolution rate of ED and cocrystals. Table 6 shows the dissolution rate constants for representative samples. The comparison of rate constants of ED cocrystals with that of ED itself reveals that the solubility rates of cocrystals are on average 1.6 times higher than that of edaravone [except ED:TMA (1:1) polymorph II]. Nevertheless, this preliminary study indicates that the dissolution rate of ED can be modified by cocrystallization. From the values of dissolution rate constants it can be seen that the prepared cocrystals can be roughly divided into the following three groups:

1. Cocrystals with significantly higher solubility rate compared to ED [ED:PC (1:1) polymorph I, ED:PC polymorph II, ED:SBA (2:1), and ED:GA (2:1) polymorph I]
2. Cocrystals with practically unchanged solubility rate [ED:CA (1:1)]

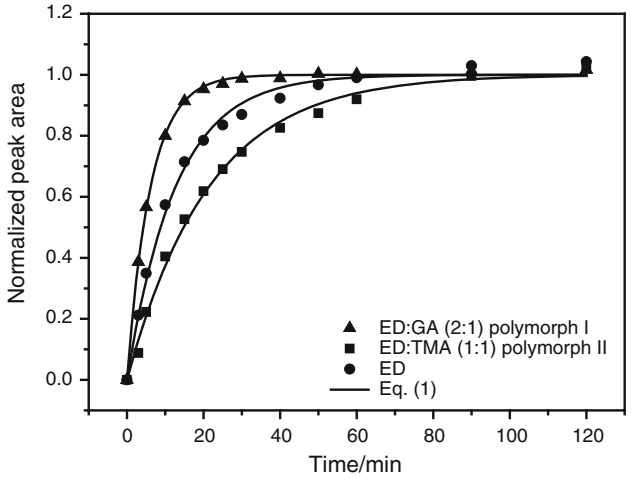

Fig. 10 Representative dissolution curves of ED:GA (2:1) polymorph I, ED:TMA (1:1) polymorph II cocrystals, and ED. *Solid line* represents non-linear fit of experimental data to Eq. (1)

Table 6 Solubility rate constants for ED and representative cocrystals

Sample	k/min^{-1}
ED	0.092
ED:PC (1:1) polymorph I	0.138
ED:PC (1:1) polymorph II	0.150
ED:GA (2:1) polymorph I	0.159
ED:CA (1:1)	0.118
ED:SBA (2:1)	0.147
ED:TMA (1:1) polymorph II	0.047

3. Cocrystals with significantly lower solubility rate compared to ED [ED:TMA (1:1) polymorph II]

It is accepted that a substance with a high melting point has strong self-interactions, and therefore low solubility [55]. This trend is approximately observed in the tested series: solubility rates of cocrystals ED:PC (1:1) polymorph I (T_{onset} = 116.4 °C), ED:PC (1:1) polymorph II (T_{onset} = 114.4 °C), ED:GA (2:1) polymorph I (T_{onset} = 154.4 °C), and ED:SBA (2:1) (T_{onset} = 158.7 °C) are about three times higher than that of ED:TMA (1:1) polymorph II (T_{onset} = 208.4 °C). As expected, the differences in the obtained solubility rates reflect the different CCFs solubilities [55], i.e., the saturated solubility of GA at 20 °C is 12 mg/cm^3, for PC 18.2 mg/cm^3, and TMA has poor solubility in water (owing to intermolecular hydrogen bonding). It may be expected that solubility of potential cocrystals of ED with more soluble acids may be higher than that of the applied phenolic acids. From this result, ED:PC and ED:GA cocrystals appear the most robust candidates; this demonstrates that using antioxidants

(phenolic acids) as CCFs yields cocrystals of ED as a crystalline, nonsolvated, highly stable solid.

Conclusion

We have shown that phenolic acids are able to cocrystallize with edaravone and also form polymorphs. Sixteen novel cocrystals have been described, with supporting analysis of FTIR and XRPD. The DSC technique was used for characterization of cocrystal polymorphs. Formation of cocrystals with different stoichiometry was observed. Each of the cocrystals was stable upon exposition to increased relative humidity and/or temperature over 8 weeks. Furthermore, dissolution studies of representative cocrystals show an alteration in solubility of edaravone with the formation of cocrystal indicating the potential for further development in this field. To summarize, cocrystal edaravone:gallic acid (2:1) polymorph II can be prepared on a large scale with robust stoichiometric control and acceptable yield, volume, and purity (chemical and solid state).

Experimental

Edaravone and CCFs were purchased from Sigma-Aldrich Ltd. and were used as received. All the samples gave microanalysis results for C ± 0.38 %, H ± 0.35 %, and N ± 0.25 %. The water content was measured by thermogravimetric analysis. All the samples showed negligible weight loss between 25 and 110 °C. Analytical grades of solvents, i.e., methanol, ethanol, acetonitrile, acetone, 2-isopropoxyethanol, methyl isobutylketone, 3-methyl-1-butanol, and *N*,*N*-dimethylformamide, were purchased from Sigma-Aldrich Ltd. Whatman nylon syringe membrane filters (0.2 μm) were used for filtration of crystallization solutions.

Preparation of cocrystals by solvent drop grinding and solvent crystallization

Cocrystals were prepared with guest compounds selected on the basis of their solubility, representative differences in structure, and range of functional groups as summarized in Table 1. The preparation included SDG and SC with a molar ratio 1:1, 2:1, or 1:2. Alternatively, these experiments were used as a rapid method of obtaining material for seeding of SC for the scale-up experiment no. 5 (Table 1).

For SDG experiments, a Retsch 200MM mixer mill, equipped with 10-cm^3 stainless steel grinding jars with two stainless steel grinding balls with a diameter of 5 or 9 mm, was used. All SDG experiments were performed with one drop of acetonitrile, dimethylformamide, or water at a frequency of 30 Hz. External temperature of the grinding jar did not exceed 30 °C.

Preparation of cocrystals by solvent crystallization was carried out in round-bottomed flasks. ED (100–200 mg) was added to the flasks in an oil bath. An adequate amount of solvent (1.5–3.5 cm^3) was added to the flask at reflux to form a solution. Then an appropriate amount of CCF was added. The solutions formed were quickly filtered through a nylon filter (0.22 μm) and then the filtrates were transferred to a 10-cm^3 flask. In some cases cosolvents (2–6.0 cm^3) were carefully added to the stirred solutions at a gentle reflux. The solutions were gently refluxed for an additional 10 min with stirring. Then the oil bath was removed and the temperature was gradually reduced to 20 °C over 0.5 h while stirring. The cooling rates for all flasks were the same. The flasks were allowed to stand at 5–10 °C for 48 h. The precipitated materials were filtered via a flask-to-flask filtration assembly using a sintered glass no. 3 funnel with vacuum. The crystals were dried under vacuum at 45 °C and stored in a desiccator. For the stability testing the materials were scaled up following the same reaction procedures.

Preparation of cocrystals via slurring

The following procedure was applied only for phenolic acids summarized in Table 2. Stoichiometric amounts of starting materials were slurried (1 cm^3 of solvent per 100 mg of starting material) to stir for 1 week at ambient temperature. The undissolved solid was isolated by vacuum filtration via a flask-to-flask filtration assembly using a sintered glass no. 3 funnel. The solids were dried under vacuum at 60 °C and stored in a desiccator. Solids were characterized using IR spectroscopy and m.p. Table 2 summarizes the cocrystals obtained in this manner.

Determination of melting points

Melting points were determined on a Boetius Nagema-type hot-stage apparatus (Rapido Wägetechnik, Radebeul, Germany). The melting point can be determined with an accuracy of 1.0 °C. The heating rate was 5 °C min^{-1}. The melting points of potential cocrystals were compared with those of ED and CCFs.

Fourier transform infrared spectroscopy

The spectra were collected on an FTIR spectrometer Impact 410-IR (Nicolet, USA). The ATR technique (diamond ATR crystal) was used with Omnic software version 5.2. A total of 50 scans were collected over the range of 4,000–400 cm^{-1}. The IR spectra of potential cocrystals were compared with those of physical mixtures of parent CCF and edaravone. The CCFs and ED were separately

gently ground before mixing to achieve the same particle size as ground cocrystal particles.

Thermal analysis

A Perkin-Elmer DSC-7 differential scanning calorimeter (DSC) with Pyris software was employed. The temperature scale was calibrated to the fusion temperatures of In, Sn, and Pb; the enthalpic scale was calibrated to the enthalpy of fusion of In. The heating rate was 10 °C min^{-1} and nitrogen was used as a purge gas.

X-ray powder diffraction

The patterns of powder samples were collected within the 2θ range 3°–51° in steps of 0.02° on a Bragg–Brentano diffractometer Philips PW1730/1050, using β-filtered CoK_{α} radiation, 40 kV/35 mA and with a scintillation detector. In order to facilitate the data interpretation, XRPD patterns of ED and CCFs were measured and compared with that of the material prepared.

Stability in solid-state and oxidative stability

Samples of cocrystals and ED were placed in open glass vials at 40 °C/75 % RH and tested periodically during 2 months by m.p. and FTIR methods. At the end of the testing period, the m.p, FTIR, and XRPD were measured for stressed samples.

For the preliminary water sorption studies, the samples and ED were milled in an agate mortar and then dried for 6 h under vacuum at 45 °C. The samples (approximately 60–120 mg) were then exposed to 55, 80, and 90 % RH for 24 h each and the weight differences for appropriate RH were calculated for dry mass. The temperature was maintained at 20 ± 2 °C; humidity was kept constant by use of saturated aqueous salt baths. The humidity and temperature were monitored using a GMH 3330 (Greisinger GmbH, Germany) with a TFS0100 probe. The cocrystal is considered non-hygroscopic if it sorbs less than 0.1 % water even at high humidities (90 % RH).

To evaluate the oxidative stability, the crystalline solids were exposed to hydrogen peroxide vapor, with RH control (25 °C/60 % RH), using the reaction chamber as described by Zhu [33]. The saturated NaCl solution was loaded into the bottom of the glass chamber. Exposure to the hydrogen peroxide vapor was from 3 days to 1 week. Samples were taken at exposure intervals and analyzed for content of edaravone using the HPLC method [56]. Degradation products were not analyzed, except sample no. 10 (Table 1) for which the LC/MS was performed with an MSD SL Ion Trap mass spectrometer with a 123 ESI and APCI source coupled with an 1100 series HPLC system.

Optical micrographs

Optical micrographs of ED, CCFs, and cocrystals were taken using the Nikon Eclipse LV 100POL polarizing microscope and analyzed using NIS Elements. Morphology of the solids was observed using a magnification ×40. The crystal diameter was measured and the number mean size for a cocrystal was calculated.

Dissolution test

The dissolution tests were conducted using a Distek Evolution 6300 dissolution system and were carried out for 1 h in 250 cm^3 of purified water at 37 °C with a paddle speed of 50 rpm. All fine samples (crystalline samples were carefully ground in an agate mortar) were agglomerated and the samples showed different wettability. In order to improve the agglomeration and wettability, the samples for the powder dissolution tests were prepared from a physical mixture of samples and α-lactose (1/20, w/w). For the dissolution test, about 5 mg of each of the fine samples (ED, cocrystals sample) was compressed into a 1.13-cm^2 disk by a hydraulic press at 90 kN for 1 min using a die with a hole 1.2 cm in diameter (Spectra-Tech, Inc., CT, USA). Dissolution experiments were run in duplicate. The stability of the solid samples after disk compression was confirmed by IR of compressed neat samples under identical conditions. Drug concentrations were determined by high-performance liquid chromatography (HPLC, Agilent Technologies 1200 system) using a DAD UV detector and a C18 column (ZORBAX Eclipse 4.6 × 100 mm 3.5-μm particle size). The dissolution samples (1 cm^3) were collected for each tablet at 3, 5, 10, 15, 20, 25, 30, 40, 50, 60, 90, and 120 min. Concentrations of ED were determined by HPLC using an external calibration curve measured before and after dissolution measurements. The wavelength for ED and cocrystals was set at 240 nm.

Acknowledgments This investigation was supported by the Slovak Research and Development Agency, grant no. APVV-121-2009 and The Agency of the Ministry of Education, Science, Research and Sport of the Slovak Republic for the Structural Funds of EU, OP RαD of ERDF by realization of the project "Evaluation of natural substances and their selection for prevention and treatment of lifestyle diseases", ITMS 26240220040 (M. Veverka, J. Gallovič, E. Švajdlenka, B. Meľuchová). Financial support from Slovak grant agency (VEGA 1/0882/13) is gratefully acknowledged (T. Dubaj, P. Šimon).

References

1. Higashi Y, Jitsuiki D, Chayama K, Yoshizumi M (2006) Recent Pat Cardiovasc Drug Discov 1:85
2. Munakata A, Ohkuma H, Nakano T, Shimamura N, Asano K, Naraoka M (2009) Neurosurgery 64:423
3. Lapchak PA (2010) Expert Opin Pharmacother 11:1753

4. Lee BJ, Egi Y, van Leyen K, Lo EH, Arai K (2010) Brain Res 1307:22
5. Kikuchi K, Takeshige N, Miura N, Morimoto Y, Ito T, Tancharoen S, Miyata K, Kikuchi C, Iida N, Uchikado H, Miyagi N, Shiomi N, Kuramoto T, Maruyama I, Morioka M, Kawahara KI (2012) Exp Ther Med 3:3
6. Yamamoto Y, Kuwahara T, Watanabe T, Watanabe K (1996) Redox Rep 2:333
7. Watanabe K, Watanabe T, Kuwahara T, Yamamoto Y (1997) J Jpn Oil Chem Soc 46:797
8. Kawai H, Nakai H, Suga M, Yuki S, Watanabe T, Saito KI (1997) J Pharmacol Exp Ther 281:921
9. Yoshinori M, Naoki M (1988) Stable injection containing 3-methyl-1-phenyl-2-pyrazolon-5-one. Jpn Patent (Kokoku) JP63-132833, 4 Jun 1988
10. Kamat CD, Gadal S, Mhatre M, Williamson KS, Pye QN, Hensley K (2008) J Alzheimers Dis 15:473
11. Jin Y, Mima T, Raicu V, Park CY, Shimizu K (2002) Neurosci Res 43:75
12. Kokura S, Yoshida N (2005) Cancer Lett 229:223
13. Zhao X, Aronowski J, Sun G, Zhang J, Strong R, Zhang Y, Grotta CJ (2005) J Neurol Sci 22:374
14. Zhang W, Sato K, Hayashi T, Omori N, Nagano I, Kato S, Horiuchi S, Abe K (2004) Neurol Res 26:342
15. Shah D, Wader GR, Mehta T (2011) Novel injectable combination. WIPO Patent WO/2011/111070, 15 Sep 2011
16. Almarsson Ö, Zaworotko MJ (2004) Chem Commun 17:1889
17. Schultheiss N, Newman A (2009) Cryst Growth Des 9:2950
18. Trask AV, Motherwell WDS, Jones W (2005) Cryst Growth Des 5:1013
19. Papadopoulos G, Boskou D (1991) J Am Oil Chem Soc 68:669
20. Rice-Evans CA, Miller NJ, Paganga G (1996) Free Radic Biol Med 20:933
21. Nakamura Y, Torikai K, Ohto Y, Murakami A, Tanaka T, Ohigashi H (2000) Carcinogenesis 21:1899
22. Babich H, Sedletcaia A, Kenigsberg B (2002) Pharmacol Toxicol 91:245
23. Childs SL (2007) Metronidazole cocrystals and imipramine cocrystals. US Patent WO2007/067727, 14 Jun 2007
24. Kavuru P, Aboarayes D, Arora KK, Clarke DH, Kennedy A, Marshall L, Ong TT, Perman J, Pujari T, Wojtas Ł, Zaworotko JM (2010) Cryst Growth Des 10:3568
25. Weyna DR, Cheney ML, Shan N, Hanna M, Wojtas L, Zaworotko MJ (2012) CrystEngComm 14:2377
26. Springuel G, Norberg B, Robeyns K, Wouters J, Leyssens T (2012) Cryst Growth Des 12:475
27. Viertelhaus M, Hilfiker R, Blatter F (2009) Cryst Growth Des 9:2220
28. Arenas-García IJ, Herrera-Ruiz D, Mondragón-Vásquez K, Morales-Rojas H, Höpfel H (2012) Cryst Growth Des 12:811
29. Friščić T, Trask VA, Jones W, Motherwell SDW (2006) Angew Chem Int Ed 45:7546
30. Zhang GG, Henry RF, Borchardt TB, Lou X (2007) J Pharm Sci 96:990
31. Childs SL, Rodriguez-Hornedo N, Reddy LS, Jayasankar A, Maheshwari C, McCausland L, Shipplett R, Stahly BC (2008) CrystEngComm 10:856
32. Li Z, Yang B-S, Jiang MO, Eriksson M, Spinelli E, Yee N, Senanayake C (2009) Org Process Res Dev 13:1307
33. Zhu D, Zhang GG, George KL, Zhou D (2011) J Pharm Sci 100:3529
34. Jayasankar A, Reddy L, Bethune SJ, Rodriguez-Hornedo N (2009) Cryst Growth Des 9:889
35. Veverka M, Šimon P, Lokaj J, Veverková E (2012) Monatsh Chem 143:65
36. Veverka M, Šimon P, Gallovič J, Jorík V, Veverková E, Dubaj T (2012) Monatsh Chem 143:1405
37. Vishweshwar P, McMahon JA, Peterson ML, Hickey MB, Shattock TR, Zaworotko MJ (2005) Chem Commun 4601
38. McMahon JA, Bis JA, Vishweshwar P, Shattock TR, McLaughlin OL, Zaworotko MJ (2005) Z Kristallogr 220:340
39. Ueto T, Takata N, Muroyama N, Nedu A, Sasaki A, Tanida S, Terada K (2012) Cryst Growth Des 12:485
40. Schultheiss N, Roe M, Boerrigter SXM (2011) CrystEngComm 13:611
41. Stahly GP (2007) Cryst Growth Des 7:1007
42. Trask AV, van de Streek J, Motherwell WDS, Jones W (2005) Cryst Growth Des 5:2233
43. Childs SL, Hardcastle KI (2007) CrystEngComm 9:364
44. Limwikrant W, Nagai A, Hagiwara Y, Higashi K, Yamamoto K, Moribe K (2012) Int J Pharm 431:237
45. Hilfiker R (ed) (2006) Polymorphism in the pharmaceutical industry. Wiley-VCH, New York
46. Aakeröy CB, Salmon DJ (2005) CrystEngComm 7:439
47. Haynes DA, Chisholm JA, Jones W, Motherwell WDS (2004) CrystEngComm 6:584
48. Balasubramani K, Muthiah PT, Lynch DE (2007) Chem Cent J 1:28
49. Kojima T, Tsutsumi S, Yamamoto K, Ikeda Y, Moriwaki T (2010) Int J Pharm 399:52
50. Zhang X-L, Ye B-H, Chen X-M (2005) Cryst Growth Des 5:1609
51. Descamps M, Willart JF, Dudognon E, Caron V (2007) J Pharm Sci 96:1398
52. Crowley KJ, Zografi G (2002) J Pharm Sci 91:492
53. Leyssens T, Springuel G, Montis R, Candoni N, Veesler S (2011) Cryst Growth Des 12:1520
54. Habgood M, Price SL (2010) Cryst Growth Des 10:3263
55. Good DJ, Rodríguez-Hornedo N (2009) Cryst Growth Des 9:2252
56. Lanchote VL, Ping WC, Santos SR (1997) Ther Drug Monit 19:705